Available online at www.sciencedirect.com
SCIENCE DIRECT
ELSEVIER
Solid State Communications 132 (2004) 19–23
solid state communications
www.elsevier.com/locate/ssc

Phase-selective cathodoluminescence spectroscopy of Er:YAG glass-ceramics

Masayuki Nishi[a,*], Setsuhisa Tanabe[b,1], Koji Fujita[a], Kazuyuki Hirao[a], Giuseppe Pezzotti[c]

[a]Department of Material Chemistry, Graduate School of Engineering, Kyoto University, Nishikyo-ku, Kyoto 615-8510, Japan
[b]Graduate School of Human and Environmental Studies, Kyoto University, Sakyo-ku, Kyoto 606-8501, Japan
[c]Department of Chemistry and Materials Engineering, Kyoto Institute of Technology, Sakyo-ku, Matsugasaki, Kyoto 606-8585, Japan

Received 12 May 2004; received in revised form 7 July 2004; accepted 9 July 2004 by H. Akai
Available online 23 July 2004

Abstract

Phase-selective excitation by a field-emission electron gun was performed for an Er^{3+}-doped $Y_3Al_5O_{12}$ (YAG) glass-ceramics, and the emission spectra due to the $^4S_{3/2} \rightarrow {}^4I_{15/2}$ transition of Er^{3+} were measured. Powder X-ray diffraction analysis revealed that a single phase of YAG was precipitated in the glass-ceramics. Field-emission scanning electron microscope (FE-SEM) images indicated that two phases existed in the glass-ceramics. There was a large difference in the intensity of cathodoluminescence (CL) between these two phases. All of the spectral peaks of the phase with higher CL intensity were attributed to the $^4S_{3/2} \rightarrow {}^4I_{15/2}$ transition of Er^{3+} in YAG crystal. The phase with lower CL intensity is considered to be composed of the glass phase including a small amount of YAG crystals. The CL from Er^{3+} in the glass phase could not be detected, implying that almost all of Er^{3+} ions are incorporated into YAG phase.

PACS: 78.60.Hk; 78.55.−m

Keywords: A. Disordered systems; D. Optical properties; E. Luminescence

1. Introduction

Luminescence spectroscopy is often utilized in order to investigate the structures of materials of interest. It is also possible to control the optical properties of the materials by modifying the structures of the materials. When a material with heterogeneous structure is examined by means of the conventional photoluminescence (PL) spectroscopy, the information about the structure is spatially averaged. Namely, the luminescence spectrum of the material involves a weighted summation over an ensemble of individual spectrum at spatially different active regions. Spatial selective spectroscopy such as cathodoluminescence (CL) is a powerful tool for resolving the spatially average spectrum, since the electron-beam broadening can be suppressed to the nanoscale region [1]. Utilizing this technique, it is possible to explore (1) the structures of heterogeneous systems such as phase-separated glasses and glass-ceramics, (2) the boundary of them, and (3) the change of local structures by some perturbations such as stress. Recently, Pezzotti estimated the nanoscale stress in

* Corresponding author. Tel.: +81-75-383-2414; fax: +81-75-383-2410.
E-mail addresses: west@collon1.kuic.kyoto-u.ac.jp (M. Nishi), stanabe@gls.mbox.media.kyoto-u.ac.jp (S. Tanabe).
[1] Tel.: +81-75-753-6832; fax: +81-75-753-6634.

0038-1098/$ - see front matter © 2004 Elsevier Ltd. All rights reserved.
doi:10.1016/j.ssc.2004.07.020

amorphous solids by use of peak-shift of luminescence due to Sm^{3+} as 'stress sensor' and by a field-emission electron gun as the excitation source for spatial selective spectroscopy [1]. In this report, CL spectra due to the $^4S_{3/2} \rightarrow {}^4I_{15/2}$ transition of Er^{3+} in the YAG glass-ceramics were measured by the phase-selective excitation using the field-emission electron gun, and the local structure around Er^{3+} was investigated.

YAG is an important structural ceramic material and can be used as potential structural fibers [2–6]. In addition, YAG doped with active ions such as rare-earth ions is extensively studied and practically used as excellent phosphor or laser materials [7–10]. Johnson et al. investigated the kinetics and pathways for crystallization of glasses with YAG composition [11]. It is expected that the spatial information about the local structure in the YAG glass-ceramics gives us some aspects if the relationship between the structure and the mechanical properties is clarified. From the optical viewpoint, it is important to investigate the local structure around rare-earth ions in each phase of the multiphase materials by phase-selective spectroscopy.

2. Experimental

Glass-ceramics were prepared from reagent-grade $CaCO_3$, Y_2O_3, Al_2O_3, SiO_2, and Er_2O_3 as starting materials. The raw materials were mixed well to produce a composition of $27.3CaO{\cdot}13.1Y_2O_3{\cdot}31.8Al_2O_3{\cdot}27.3$-$27.3SiO_2{\cdot}0.5Er_2O_3$ (mol%), and the mixture was melted in an alumina crucible at 1600 °C for 1 h. The melt was cooled to room temperature in the crucible. The glass-ceramics thus obtained will be referred to as CYAS hereafter. For comparison, a transparent glass with the composition of $34CaO{\cdot}8.5Y_2O_3{\cdot}21Al_2O_3{\cdot}36SiO_2{\cdot}0.5Er_2O_3$ (mol%) was prepared by a conventional melt-quenching method. Polycrystalline YAG doped with Er^{3+} was also prepared by a solid-state-reaction.

For phase-selective CL spectral measurements, field-emission scanning electron microscope (FE-SEM) with a lateral spatial resolution of 1.5 nm (JSM-6500F, JEOL, Tokyo, Japan), equipped with a high-sensitive detector unit (MP-32FE, Atago Bussan, Horiba Group, Tokyo, Japan) was used. Details are reported in Ref. [1].

PL spectra were measured with a Shimadzu RF5000 fluorescence spectrophotometer, in which a monochromated Xenon-lamp is used as the excitation source and a photomultiplier tube as a detector. The excitation wavelength was 378 nm for the transparent glass and 381 nm for the polycrystalline YAG, corresponding to the $^4I_{15/2} \rightarrow {}^4G_{11/2}$ transition of Er^{3+}.

X-ray powder diffraction (XRD) measurements were performed using Cu Kα radiation (XRD-6000, Shimazu, Kyoto, Japan). The diffraction angle 2θ was scanned from 10 to 80° in 0.02 increments with a scan speed of 2°/min.

3. Results

The X-ray diffraction analysis confirmed that only a single phase of YAG was precipitated in the glass-ceramics (Fig. 1). Fig. 2 shows a FE-SEM image of CYAS. Island-shaped phases (white phase) with a size of around 10 μm were observed in the other matrix phase (black phase). The CL spectra due to the $^4S_{3/2} \rightarrow {}^4I_{15/2}$ transition of Er^{3+} in a white phase and in a black phase by the phase-selective excitations are shown in Fig. 3. The spectral shapes of both phases were almost the same as each other. Notable difference was recognized in the intensity of the CL spectra between these two phases. The CL intensity of the white phase was roughly 20 times larger than that of the black phase. For comparison, a PL spectrum of Er^{3+} in a polycrystalline YAG and that in a $34CaO{\cdot}8.5Y_2O_3{\cdot}21Al_2O_3$ $\cdot 36SiO_2{\cdot}0.5Er_2O_3$ (mol%) glass are shown in Fig. 4. The glass sample showed a typical PL spectrum due to the $^4S_{3/2} \rightarrow {}^4I_{15/2}$ transition of Er^{3+} in glass materials, which had a peak at around 550 nm [13,20], while the PL spectrum of Er^{3+} in the polycrystalline YAG exhibited two emission bands at around 542 and 555 nm and a valley at around 550 nm.

4. Discussion

Fig. 5 shows the energy level diagram of Er^{3+} in YAG crystal, which is cited in Ref. [12]. Based on this diagram, possible emission wavelengths of the $^4S_{3/2} \rightarrow {}^4I_{15/2}$ transition of Er^{3+} in the YAG crystal were calculated and indicated by bars in Fig. 4. All of the PL spectral components observed in the prepared polycrystalline Er:YAG are attributed to the $^4S_{3/2} \rightarrow {}^4I_{15/2}$ transition of Er^{3+} in the YAG crystal. Comparison of Figs. 3 and 4 clearly indicates that the CL spectra of both in the white and black phases originate from the $^4S_{3/2} \rightarrow {}^4I_{15/2}$ transition of Er^{3+} in the YAG crystalline phase, although there was considerably large difference in CL intensity between these two phases as shown in Fig. 3. Considering the fact that the

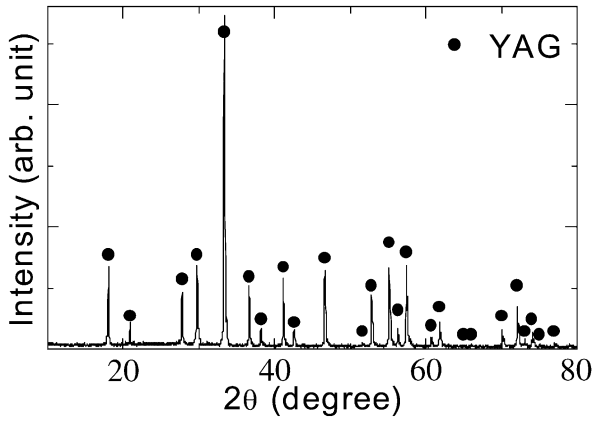

Fig. 1. XRD pattern of CYAS.

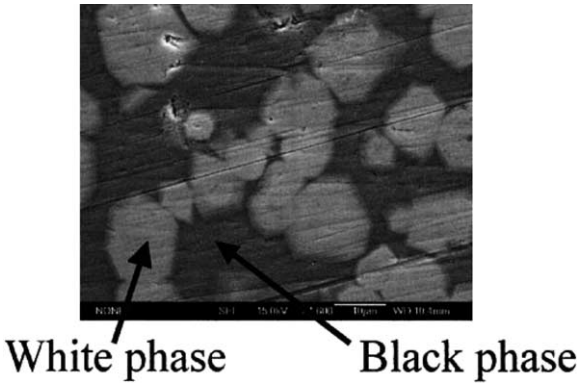

Fig. 2. FE-SEM image of CYAS.

crystalline phase of YAG is only precipitated in the glass-ceramics with the composition of $34CaO \cdot 8.5Y_2O_3 \cdot 21Al_2O_3 \cdot 36SiO_2 \cdot 0.5Er_2O_3$ (mol%) (Fig. 3), the glass phase based on the remaining CaO and SiO_2 components inevitably exists

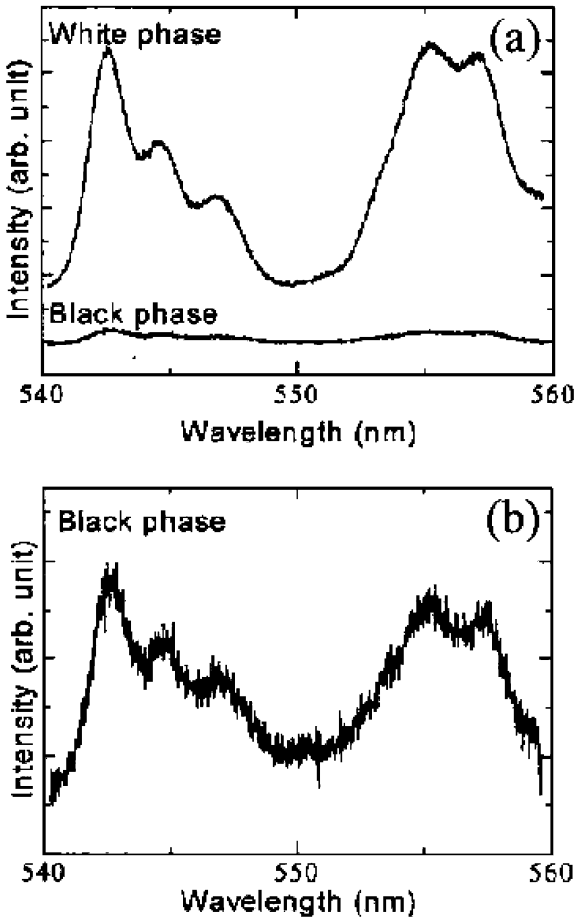

Fig. 3. (a) CL spectra due to the $^4S_{3/2} \rightarrow {}^4I_{15/2}$ transition of Er^{3+} in a white phase and a black phase obtained by the phase-selective excitation. (b) Magnified CL spectrum of Er^{3+} in a black phase.

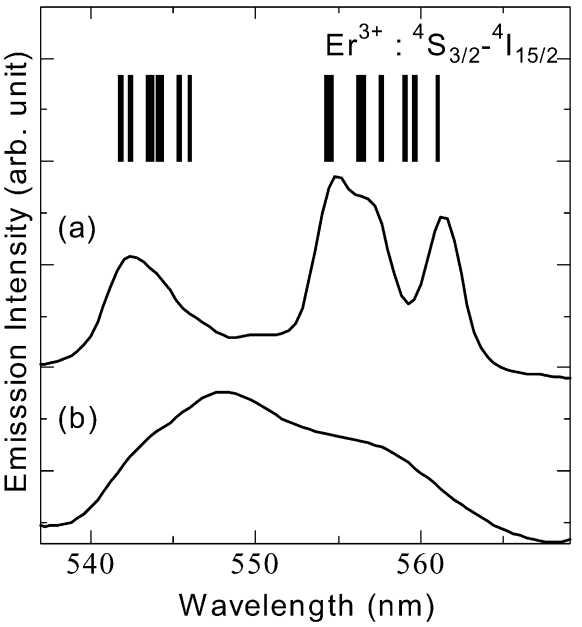

Fig. 4. PL spectrum in a polycrystalline YAG prepared by a solid-state reaction and that in a $CaO–Y_2O_3–Al_2O_3–SiO_2$ glass system. The excitation wavelength was 381 nm for the polycrystalline YAG and 378 nm for the transparent glass. The finger pattern denotes the possible emission wavelengths calculated using the values of Stark splitting of both the $^4S_{3/2}$ and $^4I_{15/2}$ levels [8].

in the glass-ceramics. For the purpose of investigating the difference between the two phases in more detail, the quantum efficiencies of the $^4S_{3/2} \rightarrow {}^4I_{15/2}$ transition of Er^{3+} both in the YAG and in the remaining silicate glass were approximately calculated. In general, the emission intensity is proportional to the quantum efficiency. The quantum

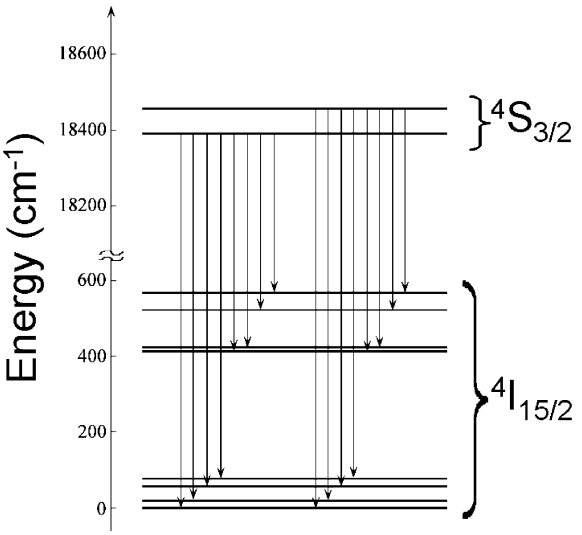

Fig. 5. Energy level diagram of the Er^{3+} in YAG crystal.

efficiency η is expressed as follows:

$$\eta = \frac{A}{A + \sum W_{NR}}, \tag{1}$$

where A (s^{-1}) is the spontaneous emission probability (radiative decay rate), and $\sum W_{NR}$ is the non-radiative decay rate. The spontaneous emission probability between an initial manifold $|(SL)J\rangle$ and a final manifold $|(S'L')J'\rangle$ is given by

$$A\left[(SL)J;(S'L')J'\right] = \frac{64\pi^4 e^2}{3h(2J+1)\lambda^3}\left\{\frac{n(n^2+2)^2}{9}S^{ed} + n^3 S^{md}\right\}, \tag{2}$$

where e is the elementrary charge, h the Planck constant, n the refractive index, and λ the mean wavelength. The S^{ed} and S^{md} are the line strengths for the electronic dipole transition and for the magnetic dipole transition, respectively. The S^{ed} is described as:

$$S^{ed}[(SL)J;(S'L')J'] = \sum_{t=2,4,6} \Omega_t |\langle (SL)J||U^{(t)}||(S'L')J'\rangle|^2 \tag{3}$$

where three terms $\langle\|U^{(t)}\|\rangle$ ($t=2, 4, 6$) are the reduced matrix elements, and the coefficients Ω_t ($t=2, 4, 6$) are the intensity parameters which are related to the crystal-fields around Er^{3+}. As for the $^4S_{3/2}\rightarrow{}^4I_{15/2}$ transition of Er^{3+}, $|\langle\|U^2\|\rangle|^2 = |\langle\|U^4\|\rangle|^2 = 0$ and $|\langle\|U^6\|\rangle|^2 = 0.2211$ [14]. Since the S^{md} is zero for the $^4S_{3/2}\rightarrow{}^4I_{15/2}$ transition, the spontaneous emission probability of the $^4S_{3/2}\rightarrow{}^4I_{15/2}$ transition of Er^{3+} is expressed as:

$$A[^4S_{3/2};{}^4I_{15/2}] = 2.74\times10^{21}\times n(n^2+2)^2\Omega_6[s^{-1}]. \tag{4}$$

Here we used the value of 18350 [cm^{-1}] as $1/\lambda$. The refractive index of the YAG crystal is around 1.8. The Ω_6 parameter of the Er^{3+} in the YAG crystal is around 0.64×10^{-20} [cm^2] [14]. Therefore, we can obtain $A = 8.6\times10^2$ [s^{-1}] as the spontaneous emission probability in the YAG phase. Based on the fact that YAG crystals are separated from the $CaO–Y_2O_3–Al_2O_3–SiO_2$ system, the main components in the residual glass phase can be CaO and SiO_2. If we assume the refractive index and Ω_6 parameter in the glass phase to be 1.6 and 0.77, respectively, which are those of a $40CaO\cdot60SiO_2$ glass [15–17], we can estimate $A = 7.0\times10^2$ [s^{-1}] in the glass phase.

In order to estimate the quantum efficiency η of the $^4S_{3/2}\rightarrow{}^4I_{15/2}$ transition of Er^{3+}, it is necessary to evaluate the multiphonon decay rate W_p from the $^4S_{3/2}$ level, since the W_{NR} is assumed to be almost equal to the W_p. According to the Miyakawa–Dexter theory [18], the W_p is expressed as:

$$W_p = W_0\exp(-\alpha\Delta E/\hbar\omega), \tag{5}$$

where ΔE is the energy gap to the next lower level and $\hbar\omega$ is the phonon energy. In the case of $^4S_{3/2}$ level of Er^{3+}, ΔE is about 2800 cm^{-1}. Based on the relationship between W_p and $\hbar\omega$ [19,20], the multiphonon decay rate of the $^4S_{3/2}$ level of Er^{3+} in the glass phase with phonon energy of around 1000 cm^{-1} due to the Si–O stretching vibration can be presumed to be 10^6 [s^{-1}], and that in the YAG phase with phonon energy of around 700 cm^{-1} [21] can be 10^4 [s^{-1}]. As a consequence, we deduced that the quantum efficiencies of the $^4S_{3/2}\rightarrow{}^4I_{15/2}$ transition of Er^{3+} in the YAG phase and the calcium silicate glass phase are about 8 and 0.07%, respectively. Table 1 summarizes the evaluated values. There can be considerably large difference in quantum efficiency between the YAG phase and the remaining silicate-based glass phase. Consequently, Er^{3+} incorporated into the YAG crystal exhibits more intense emission compared with that in the glass phase. It is thus considered that the white phase with island-shaped morphology mainly consists of Er:YAG, while the black phase is composed of the calcium silicate glass including a small amount of Er:YAG crystals. The difference of CL intensity between white and black phases is attributable to the amount of precipitated YAG crystal. Since CL spectra of Er^{3+} characteristic of glass phase are not observed, it is suggested that Er^{3+} ions tend to be incorporated into YAG phase.

5. Conclusion

CL spectra due to the $^4S_{3/2}\rightarrow{}^4I_{15/2}$ transition of Er^{3+} in the phase-selected regions were measured for the Er:YAG glass-ceramics using a field-emission electron gun. There was a considerably large difference in the CL intensity between the two phases identified by FE–SEM. Both of the CL spectra were attributable to the Er:YAG. The quantum efficiencies of the $^4S_{3/2}\rightarrow{}^4I_{15/2}$ transition of Er^{3+} both in the YAG phase and in the remaining calcium silicate-based glass phase in the glass-ceramics were calculated based on some assumptions. The calculated quantum efficiency in the YAG phase was about 100 times as large as that in the glass phase. We ascribed the difference of CL intensity between white and black phases to the amount of precipitated YAG crystal. Based on the fact that CL spectra of Er^{3+} characteristic for a glass phase are not observed, it is suggested that Er^{3+} ions tend to be incorporated into the YAG phase.

Table 1
Calculated decisive parameters for the $^4S_{3/2}\rightarrow{}^4I_{15/2}$ transition of Er^{3+} in the YAG crystal and calcium silicate glass

Phase name	Phonon energy: $\hbar\omega$ (cm^{-1})	Multiphonon decay rate: W_p (s^{-1})	Spontaneous emission probability: A (s^{-1})	QE: η (%)
Calcium silicate glass	~1000	~10^6	700	0.07
YAG crystal	~700	~10^4	860	8

References

[1] G. Pezzotti, Microsc. Anal. 2003 May.
[2] J.K.R. Weber, B. Cho, A.D. Hixson, J.G. Abadie, P.C. Nordine, W.M. Kriven, B.R. Johnson, D. Zhu, J. Eur. Ceram. Soc. 19 (1999) 2543.
[3] P.A. Doleman, E.G. Butler, Key Engng. Mater. 127–131 (1997) 193.
[4] B.H. King, J.W. Halloran, J. Am. Ceram. Soc. 78 (1995) 2141.
[5] L. Yin, Z. Zhi-Fan, J. Halloran, R.M. Laine, J. Am. Ceram. Soc. 81 (1998) 629.
[6] W.R. Blumenthal, D.S. Phillips, J. Am. Ceram. Soc. 79 (1996) 1047.
[7] A.A. Kaminskii, Crystalline Lasers: Physical Processes and Operating Schemes, CRC Press, New York, 1996. p. 13.
[8] A. Ikesue, T. Kinoshita, K. Kamata, K. Yoshida, J. Am. Ceram. Soc. 78 (1995) 1033.
[9] D. Ravichandran, R. Roy, A.G. Chakhovskoi, C.E. Hunt, W.B. White, S. Erdei, J. Lumin. 71 (1997) 291.
[10] M.S. Scholl, J.R. Trimmer, J. Electrochem. Soc. 133 (1986) 643.
[11] B.R. Johnson, Waltraud M Kriven, J. Mater. Res. 16 (6) (2001) 1795.
[12] A.A. Kaminskii, Crystalline Lasers: Physical Processes and Operating Schemes, CRC Press, New York, 1996. p. 188.
[13] S. Tanabe, S. Yoshii, K. Hirao, N. Soga, Phys. Rev. B 45 (1992) 6420.
[14] A.A. Kaminskii, Crystalline Lasers: Physical Processes and Operating Schemes, CRC Press, New York, 1996. p. 299.
[15] O.V. Mazurin, M.V. Streltsina, T.P. Shvaiko-Shvaikvskaya, Physical Science Data 15 Handbook of Glass Data Part A, Elsevier, New York, 1983. p. 481.
[16] O.V. Mazurin, M.V. Streltsina, T.P. Shvaiko-Shvaikvskaya, Physical Science Data 15 Handbook of Glass Data Part C, Elsevier, New York, 1987. p. 772.
[17] H. Takebe, Y. Nageno, K. Morinaga, J. Am. Ceram. Soc. 78 (5) (1995) 1161.
[18] T. Miyakawa, D.L. Dexter, Phys. Rev. B 1 (1970) 2961.
[19] C.B. Layne, W.H. Lowdermilk, M.J. Weber, Phys. Rev. B 16 (1977) 10.
[20] S. Tanabe, H. Hayashi, T. Hanada, N. Onodera, Opt. Mater. 19 (2002) 343.
[21] G.M. Zverev, G.Y. Kolodnyi, A.M. Onishchenko, Sov. Phys. JETP 33 (1971) 497.